Cu_2Sb THIN FILM ELECTRODES PREPARED BY PULSED LASER DEPOSITION

Seung-Wan Song,[a] Ronald P. Reade,[a] Elton J. Cairns,[a]
John T. Vaughey,[b] Michael M. Thackeray[b]
and Kathryn A. Striebel[a]

[a]Environmental Energy Technologies Division
Ernest Orlando Lawrence Berkeley National Laboratory,
Berkeley, California 94720, USA
[b]Chemical Engineering Division, Argonne National Laboratory,
Argonne, Illinois 60439, USA

ABSTRACT

Thin films of Cu_2Sb have been prepared on stainless steel and copper substrates with a pulsed laser deposition technique at room temperature. The cyclability was excellent for the voltage range 0.0 - 1.2 V vs. Li for Cu_2Sb films on copper, with capacities greater than 200 mAh/g for more than 50 cycles, whereas electrodes using stainless steel substrates showed a rapid capacity loss. Greater cycling stability was obtained when cells were cycled over the voltage range 0.65-1.4 V. The superior performance for Cu_2Sb films on copper may be due to increased participation of the extruded copper in the functioning of the electrode, whereas extruded copper on stainless steel may become locally isolated.

INTRODUCTION

Sb-containing intermetallic compounds such as InSb (1-3) Cu_2Sb (4), SnSb (5,6), have recently been suggested as alternative negative electrodes to graphite in rechargeable lithium batteries. Two general advantages of intermetallic electrodes are 1) their ability to operate several hundred millivolts above metallic lithium, which improves cell safety, and 2) volumetric capacities that are significantly larger than the 820 mAh/cm^3 for graphite. For example, the theoretical volumetric capacity of tetragonal Cu_2Sb (*P4/nmm*) (4, 7) is 2749 mAh/cm^3 due to its high crystallographic density of 8.51 g/cm^3. In contrast to other intermetallics, such as InSb, only the Sb atoms in Cu_2Sb have an affinity for lithium. The reaction between pure Sb metal and lithium to form Li_3Sb (3, 8) produces a large specific capacity and unfortunately is accompanied by a significant volume change of 137% which can cause electrochemical-mechanical disintegration of particles during cycling. However, intermetallic compounds with Sb tend to show improved reversibility during cycling. It has been reported that lithium insertion into the Cu_2Sb structure causes a transformation to the cubic intermediate Li_2CuSb (*F-43m*) (9) with a [CuSb] zinc-blende framework by extruding 50% of the Cu atoms from Cu_2Sb. This reaction is followed by the formation of cubic Li_3Sb (*Fm3m*) (10), *via* $Li_{2+x}Cu_{1-x}Sb$, on complete extrusion of Cu. The extrusion of metallic Cu, which shows no significant

reactivity with lithium has been shown to be largely reversible if copper current collectors are used. For example, powder electrodes of Cu_2Sb in lithium coin cells have shown stable cycling behavior (25 cycles) over the full voltage range 0.0-1.2 V, delivering 290 mAh/g (4), which is close to the theoretical capacity of a Cu_2Sb electrode (323 mAh/g). For longer term cycling, the irreversibility of the reaction can be inhibited, or at least restricted, if the voltage window is limited to the region of the Cu_2Sb-Li_2CuSb solid solution. This behavior has been attributed to the fact that the lithiated intermediate composite has a strong structural relationship to that of the parent electrode (4). Clearer information about the performance of low conductivity materials can often be obtained when they are in thin film form because conductive additives and binders are not required (11-13). Geometrically well-defined electrodes can simplify the system by eliminating complications from the carbon and binder that are necessary for powder-based electrodes. Furthermore, nanometer-scale electrode materials that can be homogeneously deposited are of particular interest because they can be more tolerant to structural-mechanical changes during electrochemical cycling (13-15).

In this work, nanometer-scale thin films of Cu_2Sb, prepared on stainless steel (SS) and copper substrates by pulsed laser deposition (PLD), have been used as a model system to study the electrochemical properties and reaction mechanisms of intermetallic electrodes in the absence of carbon and binder materials. Various voltage windows for cycling have been used to determine reversible cycling regions. The electrochemical behavior of films is compared with that of powder electrodes.

EXPERIMENTAL

The Cu_2Sb films were prepared on 6 mm diameter (3 mm thick) SS disks and Cu foil (25 μm thick) substrates with PLD at room temperature with 10 minutes deposition in 10 mtorr of Ar. Deposition was accomplished using a XeCl eximer laser with an energy density of 3-4 mJ/cm^2 at 10 Hz impinging on a target pressed from ball-milled Cu_2Sb powder. The distance between the target and the substrates was approximately 5 cm. The SS substrates were mounted on a Si wafer, partially masking the Si during PLD. The film on the Si was used for film thickness evaluation, whereas the films on SS were reserved for electrochemical measurements. The as-prepared films appeared shiny and light blue in color. Film thickness was evaluated by tilting a partly broken piece of film-coated wafer in a field emission scanning electron microscope (Jeol 6340 FESEM) to see the cross-section. The crystal structure of the film was identified by X-ray diffraction using an X-ray diffractometer (Siemens D5000) with Ni filtered Cu Kα radiation at 40 kV and 30 mA, and a scan rate of 1.5° / min from 20 to 60° 2θ with 0.05° steps.

The electrochemical cell, containing the Cu_2Sb films on SS disks with a Li reference electrode (RE) and a Li counter electrode (CE), has been described previously (12). The films on stainless steel and Cu substrates, henceforth denoted as Cu_2Sb/SS and Cu_2Sb/Cu respectively, were cycled at a constant current of 35μA/cm^2 between 0.0 or 0.1 V and 1.2 V vs. Li/Li^+, using an Arbin Battery Cycler (College Station, TX). Films were also cycled between 0.1-0.7 V and 0.65-1.4 V for voltage window experiments. For comparison, an electrode containing 70% Cu_2Sb powder, 20% carbon (10% SFG-6 graphite and 10% acetylene black) and 10% PVDF binder on Cu foil was cycled at 100

$\mu A/cm^2$ over the ranges of 0.0-1.2 V and 0.65-1.4 V. Both the Cu_2Sb/Cu films and the Cu_2Sb powder electrodes were cycled in Swagelok® cells with a Li RE and CE, and a Celgard 2300 separator. All electrodes were tested in 1M $LiPF_6$/EC+DEC (1:1) electrolyte (EM Industries).

RESULTS AND DISCUSSION

Film Characterization

The FESEM cross-section image of a Cu_2Sb/SS film, shown in Fig. 1(a), reveals a film thickness of 26 nm. The film appeared smooth and not well crystallized. The Cu_2Sb/Cu film was not prepared on the Si wafer, so the thickness of this film was estimated to be 289 nm from deposition parameters. In the surface SEM image, shown in Fig. 1(b), the thicker Cu_2Sb/Cu film appears to be more crystalline than the Cu_2Sb/SS film, with crystallites on the order of 0.25 μm. In an X-ray diffraction pattern of the Cu_2Sb/SS film, which shows limited crystal growth, only a few of the major reflections of the tetragonal Cu_2Sb structure are evident (Fig. 2). It is possible that during the deposition process, X-ray amorphous phases (such as Sb metal, which is more volatile than Cu) were deposited on the substrate thereby making it difficult to calculate the precise theoretical capacity of the electrode. Note that some peaks of the characteristic Cu_2Sb pattern, located at approximately 42 and 52° 2θ, overlap with strong peaks from the stainless steel substrate at approximately 43 and 52^o 2θ , respectively. It was not possible to obtain an acceptable XRD pattern of the Cu_2Sb/Cu electrode because of difficulties in placing a sufficiently flat Cu_2Sb/Cu film in the diffractometer.

Constant Current Cycling of Cu_2Sb/SS Films

The initial galvanostatic charge-discharge voltage profiles of cells with Cu_2Sb/SS films cycled over a wide voltage range (0.1-1.2 V) and over a limited range (0.65-1.4 V) are shown in Figs. 3(a) and 3(b), respectively. In a later paper we will compare the half-cell and full-cell performance of these anode materials. For this reason, we define charge as the cathodic addition of Li to Cu_2Sb. The integrated *discharge* (anodic) capacities are shown in Fig. 3(c). These values represent minimum capacities because the weight of Cu_2Sb in the film was estimated from the film thickness and crystallographic density. These data clearly show the superior cycling stability of Cu_2Sb over the limited voltage window (0.65-1.4 V). The plateaus in the potential profiles are more clearly distinguished in the calculated differential capacity plots shown in Fig. 4a and b. In Fig. 4a (0.1-1.2 V), the initial cathodic curve shows small peaks at 1.85 and 1.5 V that have been attributed to the reduction of the surface oxide (4). The set of large peaks near 0.8 V are attributed, in part, to the reduction of electrolyte components, forming a conductive layer and, in part, to lithium insertion into Cu_2Sb, forming the intermediate lithiated zinc-blende-type phase, Li_2CuSb. The potential of this first lithiation is shifted cathodically from the expected value of 0.93 V (4). The shape of the peak and the fact that it appears at this potential only on the first cycle suggest a nucleation-type phenomenon, perhaps for the nucleation of the extruded Cu. This process is followed by a cathodic peak at 0.6 V that can be attributed to the simultaneous lithium insertion and Cu extrusion forming first a solid solution, $Li_{2+x}Cu_{1-y}Sb$, and thereafter the Li_3Sb alloy upon complete lithium

insertion/copper extrusion. On the reverse process, the two anodic peaks observed near 1.0 V are attributed to the regeneration of the Cu_2Sb-type structure via the same intermediate lithiated zinc-blende phase (4). On the following cycle, the two cathodic peaks are shifted to 0.93 and 0.5 V. On further cycling, these peaks remain at approximately the same potential, gradually disappearing by the 25th cycle. In Fig. 4(b), the Cu_2Sb/SS film, when cycled in the limited voltage window (0.65-1.4 V) shows, on the first cycle, the same cathodic displacement of the initial Li insertion process. Both anodic and cathodic peaks are observed over 90 cycles suggesting that the capacity retention is improved by limiting the voltage range and restricting the extent of Cu-extrusion, consistent with previous reports (4). During this electrochemical process, the electrode structure maintains a *fcc* array of Sb. The process appears to become more irreversible with continued cycling, possibly due to an increased resistivity in the film due to loss of contact of the extruded copper particles with the parent intermetallic structure.

The capacity plot in Fig. 3(c) confirms that the limited voltage range, 0.65-1.4 V, was effective in improving capacity retention. For this range, a capacity of 200-300 mAh/g was achieved for 50 cycles. However, a capacity of 300 mAh/g exceeds that which is theoretically allowed for the reaction to produce Li_2CuSb (215 mAh/g). Therefore, this finding strongly suggests that the PLD thin-film electrodes may contain an undetectable Sb component, because the reaction of Li with Sb to form Li_3Sb provides a larger theoretical capacity (661 mAh/g). A wider voltage-range cycling (0.1-1.2 V) resulted in rapid capacity loss within ten cycles. One film was also cycled over a lower voltage range (0.1-0.7 V) in order to restrict cycling to the Li_2CuSb - Li_3Sb alloy reaction. This voltage regime indicated inferior cycling stability compared to the other voltage ranges described above, and showed a rapid and continuous decline in the capacity delivered by the electrode.

Constant Current Cycling of Cu_2Sb/Cu Films

Cu_2Sb/Cu films were cycled over two similar voltage ranges (0.0-1.2 V and 0.65-1.4 V). Differential capacity plots of the voltage profiles are shown in Figures 5(a) and 6(a); for comparison, differential capacity plots of Cu_2Sb powder electrodes are included in Figures 5(b) and 6(b), respectively. The shift that was observed in the first cathodic lithiation of a Cu_2Sb/SS electrode, is not observed for the Cu_2Sb/Cu films. Both film and powder electrodes show initial cathodic processes close to 0.93 V, which was attributed to the phase transformation that occurs when Cu_2Sb is lithiated to form Li_2CuSb. As with the Cu_2Sb/SS films, this process is followed by a peak near 0.6-0.7 V which was attributed to further lithium insertion into, and extrusion of Cu from, Li_2CuSb to form Li_3Sb (4). Capacity from the three anodic plateaus between 0.8-1.0 V is attributed to the delithiation of Li_3Sb, accompanied by the reincorporation of Cu into the Sb array and the regeneration of the Cu_2Sb-type structure. As with the Cu_2Sb/SS film cycled over the wide voltage window (0.0-1.2 V), the anodic and cathodic peaks of the Cu_2Sb/Cu film disappear by the 25th cycle, indicating a loss of discrete crystalline phases (Fig. 5a), whereas when the voltage window is restricted to 0.65-1.4 V, distinct peaks in the differential capacity plots appear to indicate a more ordered structure in the electrode (Fig. 6a). It is possible that the large volume expansion (42%) of the Sb array, which accompanies the transformation from Cu_2Sb to Li_3Sb, may lead to the isolation of the Cu particles, and the consequent formation of Sb nanoparticles on charge, during extended

cycling. In this instance, Sb nanoparticles would react directly with lithium, thereby contributing to the capacity and reversibility of the reaction; this process occurs at approximately 1.0 V vs. Li (3).

The differential capacity plots of the Cu_2Sb powder electrode also show a loss of definition for the voltage range 0.0-1.2 V over 50 cycles (Fig. 5(b)). However, in this case, the plots show distinct peaks at potentials below 0.3 V vs. Li/Li^+, which were attributed to Li insertion into the graphite (SFG-6) component of the electrode. Plots of capacity vs. cycle number for the thin-film and powder Cu_2Sb electrodes are provided in Figure 7. For the voltage range 0.65-1.4 V, the Cu_2Sb powder electrode shows superior cycling (Fig. 7b), both in terms of delivered capacity and the rate capacity fade, which was 0.31% per cycle compared to 1.10% per cycle for the Cu_2Sb/Cu film electrode. Of particular note, is that the powder electrode delivers a very steady 135 mAh/g over this voltage range which corresponds to the reaction of approximately 1.3 Li per Cu_2Sb, and to the reversible phase transformation between Cu_2Sb and $Li_{1+x}Cu_{2-y}Sb$. By contrast, for the voltage range 0.0-1.2 V, the Cu_2Sb/Cu film electrode shows superior performance for the first 100 cycles (Fig. 7a).

Although further work is required to optimize the electrochemical performance of thin-film Cu_2Sb electrodes, it is believed that a Cu substrate is favored over a SS substrate for the following reasons. Once aggregation or crystallization of the extruded Cu particles and phase separation occur during cycling, it is anticipated that it would not be easy to reverse the electrochemical process, and rapid capacity fade can be expected as a result of the loss of both particle contact and matrix conductivity. In this context, the reversibility of Cu_2Sb/Cu film electrodes can be attributed to a homogenous dispersion of nano-sized Cu particles that are extruded from the $Li_xCu_{2-y}Sb$ electrode and deposited onto the Cu substrate. It is proposed that in such an instance, the extruded Cu would participate more actively in the functioning of the electrode, particularly with respect to supporting electronic conductivity, whereas the copper deposited onto a SS substrate may become locally isolated. In this respect, it is anticipated that intermetallic anodes with an inactive metal component may, in general, be best prepared on a substrate of the same metal if the inactive metal component can be extruded without any destructive structural rearrangement of the host electrode. This active participation has already been demonstrated for Cu in the case of Cu_6Sn_5/Cu films (16).

CONCLUSIONS

Thin PLD films of Cu_2Sb/Cu electrodes showed relatively stable cycling behavior over the voltage range of 0.0-1.2 V, but enhanced stability over the more limited voltage window (0.65-1.4 V vs. Li/Li^+). Although Cu_2Sb/SS films showed good cycling stability over the narrower voltage range, they lost capacity rapidly if cells were cycled over the range 0.1-1.2 V. The cycling performance of Cu_2Sb electrodes was, therefore, primarily dependent on the substrate and voltage window used. The superior performance of thin-film Cu_2Sb electrodes deposited onto a Cu substrate compared to a SS substrate was attributed to 1) the higher electronic conductivity of Cu, and 2) greater compatibility between the extruded Cu and the substrate, leading to greater electronic connectivity

between the extruded Cu and the remaining lithiated intermetallic component of the electrode.

ACKNOWLEDGMENTS

This work was supported by the Office of Energy Research, Basic Energy Sciences, Chemical Sciences Division of the Department of Energy under contract No. DE-ACO3-76SF00098.

REFERENCES

1. J. T. Vaughey, J. O'Hara and M. M. Thackeray, *Electrochem. Solid State Chem*., **3**, 13 (2000).
2. C. S. Jonhson, J. T. Vaughey, M. M. Thackeray, T. Sarakonsri, S. A. Hackney, L. Fransson, K. Edström and J. O. Thomas, *Electrochem. Commun*., **2**, 595 (2000).
3. K. C. Hewitt, L. Y. Beaulieu and J. R. Dahn, *J. Electrochem. Soc*., **148** A402 (2001).
4. L. M. L. Fransson, J. T. Vaughey, R. Benedek, K. Edström, J. O. Thomas and M. M. Thackeray, *Electrochem. Commun*., **3**, 317 (2001).
5. J. Yang, M. Winter and J. O. Besenhard, *Solid State Ionics*, **90**, 281 (1996).
6. H. Li, L. Shi, W. Lu, X. Huang and L. Chen, *J. Electrochem. Soc*., **148**, A915 (2001).
7. W. B. Pearson, *Z. Kristall*., **171**, 23 (1985).
8. J. Wang, I. D. Raistrick and R. A. Huggins, *J. Electrochem. Soc*., **133**, 457 (1986).
9. H. Paulty, A. Weiss and H. Witte, *Z. Metallk*., **59**, 47 (1968).
10. G. Brauer and E. Zintl, *Z. Phys. Chem*., **37**, 323 (1937).
11. K. A. Striebel, C. Z. Deng, S. J. Wen and E. J. Cairns, J. *Electrochem. Soc*., **143**, 1821 (1996).
12. K. A. Striebel, A. Rougier, C. R. Horne, R. P. Reade and E. J. Cairns, *J. Electrochem. Soc*., **146**, 4339 (1999).
13. S. W. Song, K. A. Striebel, R. P. Reade, G. A. Roberts and E. J. Cairns, *J. Electrochem. Soc*., **150**, A121 (2003).
14. H. Li, X. Huang, L. Chen, Z. Wu and Y. Laing, *Electrochem. Solid-State Lett*., **2**, 547 (1999).
15. S. Grugeon, S. Laruelle, R. Herrera-Urbina, L. Dupont, P. Poizot and J-M. Tarascon, *J. Electrochem. Soc*., **148**, A285 (2001).
16. N. Tamura, R. Ohshita, M. Fujimoto, S. Fujitani, M. Kamino and I. Yonezu, *J. Power Sources*, **107**, 48 (2002).

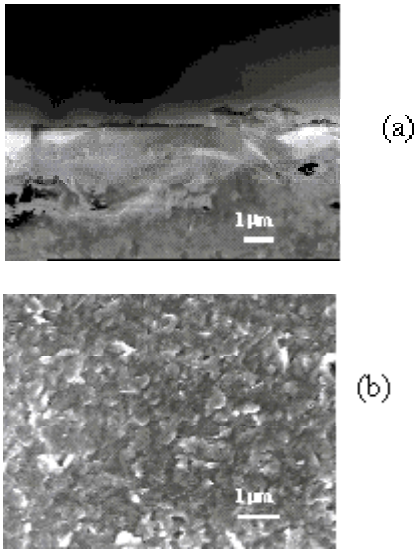

Figure 1. SEM images for (a) cross-section of Cu_2Sb/SS film and (b) surface morphology of Cu_2Sb/Cu film.

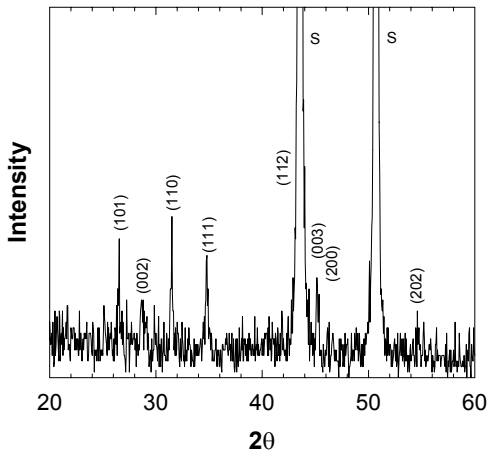

Figure 2. X-ray diffraction pattern of Cu_2Sb/SS PLD film prepared at room temperature; S notes the peaks from the stainless steel substrate.

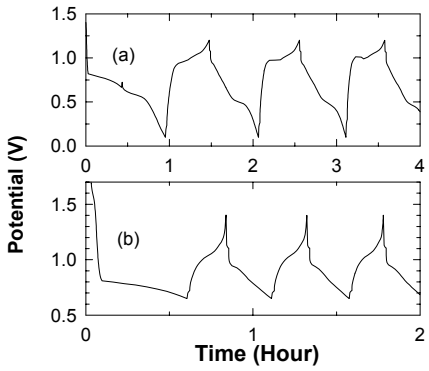

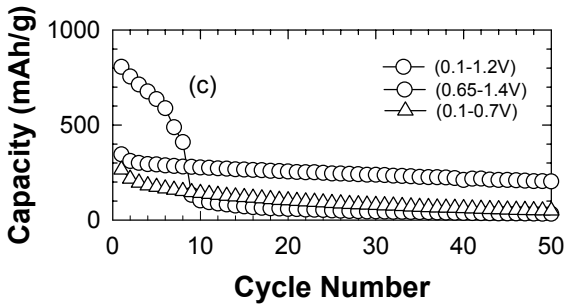

Figure 3. Constant current (35 μA/cm^2) cycling for Cu_2Sb/SS films in three voltage windows; voltage profiles (a) 0.1-1.2 V (-●-), (b) at 0.65-1.4 V (-○-), (c) discharge (anodic) capacities 0.1-0.7V (-Δ-).

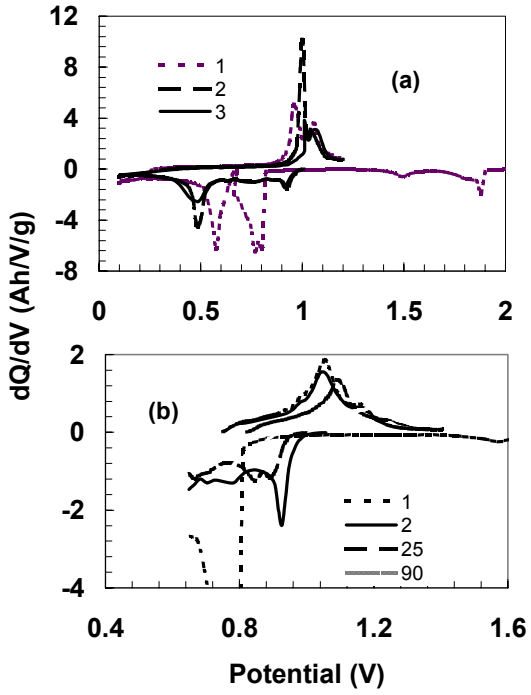

Figure 4. Differential capacity plots for Cu_2Sb/SS film in the voltage range of (a) 0.1-1.2V and (b) 0.65-1.4V for different cycles.

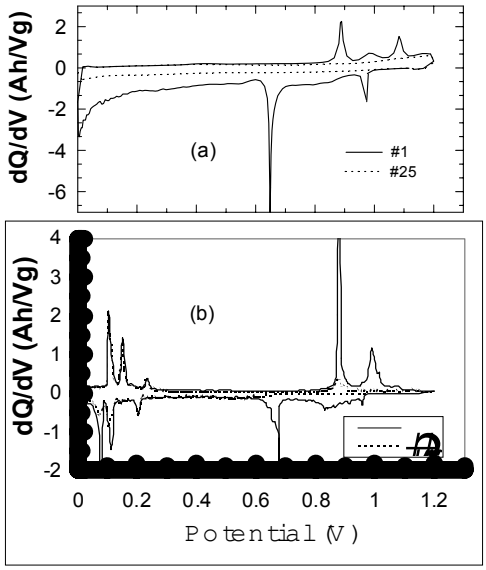

Figure 5. Differential capacity plots for (a) Cu_2Sb/Cu PLD and (b) Cu_2Sb powder electrodes, 0.0 to 1.2 V vs. Li/Li^+.

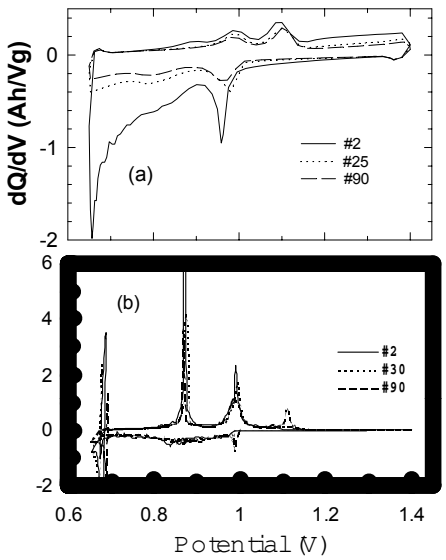

Figure 6. Differential capacity plots for (a) Cu_2Sb/Cu film and (b) Cu_2Sb powder electrode, 0.65-1.4 V vs. Li/Li^+

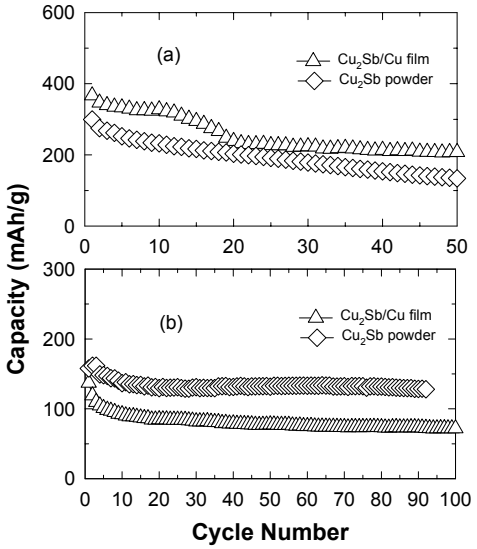

Figure 7 Comparative plots of specific discharge capacities obtained by cycling Cu_2Sb/Cu film (-Δ-) and Cu_2Sb powder (-◆-) at (a) 0.0-1.2V and (b) 0.65-1.4V.